Comparison of Chest Dual-Energy Subtraction Digital Tomosynthesis and Conventional Digital Tomosynthesis for the Detection of Simulated Pulmonary Nodules with Calcifications: Phantom Study

Tsutomu Gomi*,[1], Masahiro Nakajima[2] and Hiroki Fujiwara[2]

[1]*School of Allied Health Sciences, Kitasato University, Sagamihara, Kanagawa, Japan;* [2]*Dokkyo Medical University Hospital, Koshigaya, Saitama, Japan*

Abstract: To compare the effectiveness of chest dual-energy subtraction digital tomosynthesis (DES-DT) with that of conventional digital tomosynthesis for the detection of calcifications superimposed over simulated pulmonary nodules. A DES-DT system with pulsed X-rays and rapid kV switching was used to examine calcifications in simulated pulmonary nodules. Low-voltage, high-voltage, and soft-tissue or bone-subtracted tomograms of the desired layer thicknesses were reconstructed from the image data acquired during a single tomographic scan, bone-subtracted images, and a scan angle of 40°. Our analysis took into account the signal-to-noise ratio (SNR) of the different degrees of calcification in the simulated pulmonary nodules. For DES-DT, the SNR for the simulated pulmonary nodules increased about 63%. Based on the results of receiver operating characteristic performance analysis, the detection ability of our DES-DT was significantly better than that of conventional digital tomosynthesis ($P < 0.03$). The study results confirmed with a further study to assess influence of reconstruction and filtering for detection of simulated nodules. DES-DT provided greater sensitivity than conventional digital tomosynthesis.

Keywords: Tomosynthesis, dual-energy subtraction, pulmonary nodules.

1. INTRODUCTION

Lung cancer is currently the leading cause of cancer death and continues to be an increasing cause of death worldwide. Due to its high sensitivity, normal-dose helical computed tomography (CT) is currently considered the gold standard for lung cancer detection. Early reports indicate that low dose helical CT has promise to detect early lung cancer and thus decrease morbidity [1]. These methods offer much higher sensitivity and specificity than chest radiography as it is currently practiced. Chest radiography has been shown to have relatively low sensitivity for detection of pulmonary nodules. This poor sensitivity for chest radiography precludes its use as a screening modality, despite the low cost, low dose, and wide distribution of devises.

Dual energy subtraction (DES) imaging has been proposed and investigated by many researchers as a means of reducing the impact of anatomic 'noise' on detection of disease in chest radiography. DES involves making two radiographic projections of the patient using different energy x-ray beams. By exploiting the difference in the energy dependence of attenuation between bone and soft tissue, the contrast of the bone can be reduced producing a soft-tissue only image, and the contrast of the soft tissue can be reduced to produce a bone image [2]. CT scanners were used in Scout-view mode [3], and even film has been proposed as dual-energy receptor [4]. Recent Computed Radiography

(CR) systems have been hampered by poor subtraction effectiveness, workflow inconveniences, and Detective Quantum Efficiency (DQE) limitations of the CR technology.

In the differentiation of benign and malignant pulmonary masses, 2 radiographic findings give indications of a benign lesion: the presence of calcifications in the mass, and stability of the mass [5-9]. A benign pattern of the calcifications has been considered necessary to exclude malignancy [6, 10-13]. In the evaluation of diffusely disseminated pulmonary nodules, identification of diffusely disseminated pulmonary nodules, identification of calcifications in the nodules has been helpful in limiting the differential diagnosis [14]. Conventional radiography and conventional tomography have been used to detect calcifications, but they have been largely replaced by CT [7-8]. However, CT has several inherent problems, including motion artifacts and a variety of reconstruction algorithms used different scanners. Despite recent developments in CT techniques, difficulties remain, such as shifting of the slice level in thin-section CT images acquired during different breaths, and difficulty in clarifying the characteristics and distribution of calcifications relative to soft tissue components of the mass. Dual-energy digital radiography has been found useful in detecting calcifications [6, 9, 15-18]. Projection images acquired using DES techniques, however, suffer from the problem of overlap of anatomic features (e.g., calcifications superimposed over the ribs or spine).

Interest in tomosynthesis and its clinical applications has been revived by recent advances in digital X-ray detector. A

*Address correspondence to this author at the School of Allied Health Sciences, Kitasato University, Kitasato 1-15-1, Minami-ku, Sagamihara, Kanagawa 252-0373, Japan; Tel: +81 (0)42-778-9617; Fax: +81 (0)42-778-9628; E-mail: gomi@kitasato-u.ac.jp

review of tomosynthesis has been given by Dobbins *et al* [19]. Conventional tomography technology provides planar information of an object from its projection images. In tomography, an X-ray tube and an X-ray film receptor lie on either side of the object. The relative motion of the tube and film is predetermined based on the desired location of the in-focus plane. A single image plane is generated by a scan and multiple scans may be required to provide a sufficient number of planes to cover the selected structure in the object. Tomosynthesis acquires only one set of discrete X-ray projections that can be used to reconstruct any plane of the object retrospectively. The technique has been investigated in angiography, chest imaging, hand-joint imaging, pulmonary imaging, dental imaging, and breast imaging [19].

In this paper, we focus on addressing the problems associated with thin-sliced CT scanning and projection-type DES images, we have developed a DES digital tomosynthesis system (DES-DT). Here we report initial studies on the comparison of the chest DES-DT with that of conventional digital tomosynthesis for the detection of calcifications superimposed over simulated pulmonary nodules.

2. MATERIALS AND METHODS

2.1. DES-DT System

The DES-DT system (SonialVision Safire II, Shimadzu Co., Kyoto, Japan) consisted of an X-ray tube with a 0.4 mm focal spot and a 432 mm × 432 mm amorphous selenium digital flat-panel detector with a pixel size of 150 × 150 μ. The motion of the collimator is synchronized with tube motion constant misregistration of low kVp and high kVp images. In DES-DT, pulsed X-ray exposures are used with rapid switching between low energy (60 kVp) and high energy (120 kVp). In conventional digital tomosynthesis, pulsed X-ray exposures are used with high energy (120 kVp). Tomography is performed with linear tomographic

movement of the system, with a scan time of 6.4 s and a swing angle of 40°. Thirty-seven low- and high-voltage projection images are sampled during a single tomographic pass. These images are sampled using a matrix size of 2880 × 2880 by 12 bits and are used to reconstruct low- and high-voltage tomograms at any desired height. Bone or soft tissue tomograms are produced by weighted subtraction for each different absorption coefficient (Fig. **1**). Each projection image is acquired at 200 mA and 20 to 25 ms exposure time for low voltage X-rays, and at 200 mA and 25 ms or less for high-voltage X-rays. An anti-scatter grid was used (focused type, grid ratio 12:1). The tomosynthesis images were reconstructed by using filtered back projection [20].

2.2. Specification of Phantom and Simulated Pulmonary Nodules

Chest Phantom (Fig. **2**)	Type N1 (Kyoto Kagaku Co., Tokyo, Japan)
Simulated pulmonary nodules (Fig. **2**)	simulated of ground glass opacity (GGO) type
	5 mmϕ
	-630 Hounsfield Unit, spheres type
	Same diameter and composition
Calcification	hydroxyapatite (powder type)
Amount of calcification	small (100mg/ml)
	medium+ (200mg/ml)
	medium ++ (300mg/ml)
	large (400mg/ml)

The simulated pulmonary nodules were arranged in the lung region. The simulated pulmonary nodules, the relationship between the radiation attenuation properties of glass and real pulmonary nodules were correlated. The
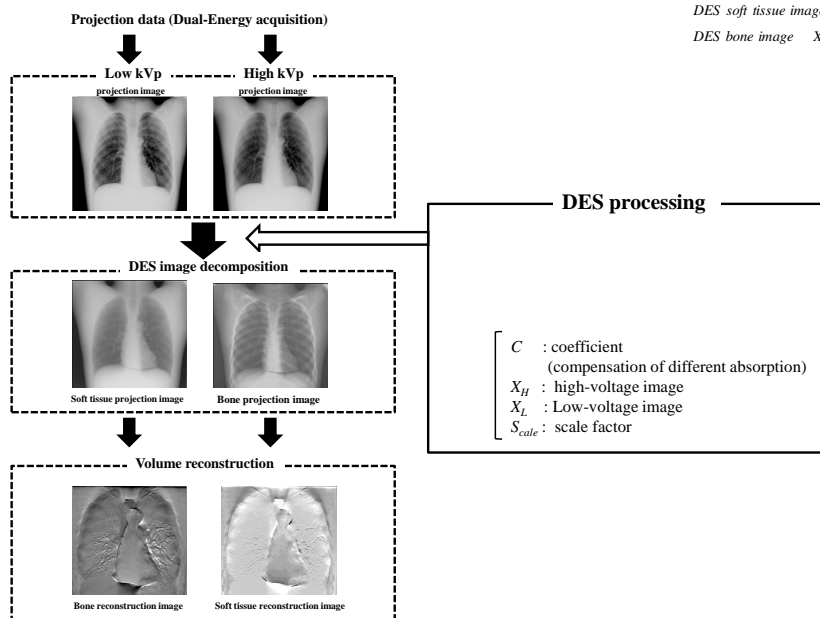
DES soft tissue image $C\ X_H\ X_L\ S_{cale}$
DES bone image $X_L\ C\ X_H\ S_{cale}$

DES processing

$$
\begin{bmatrix}
C & : \text{coefficient} \\
& \quad \text{(compensation of different absorption)} \\
X_H & : \text{high-voltage image} \\
X_L & : \text{Low-voltage image} \\
S_{cale} & : \text{scale factor}
\end{bmatrix}
$$

Fig. (1). Illustration of the imaging sequence and processing of dual-energy acquisition.

5mm φ

Simulated pulmonary nodule
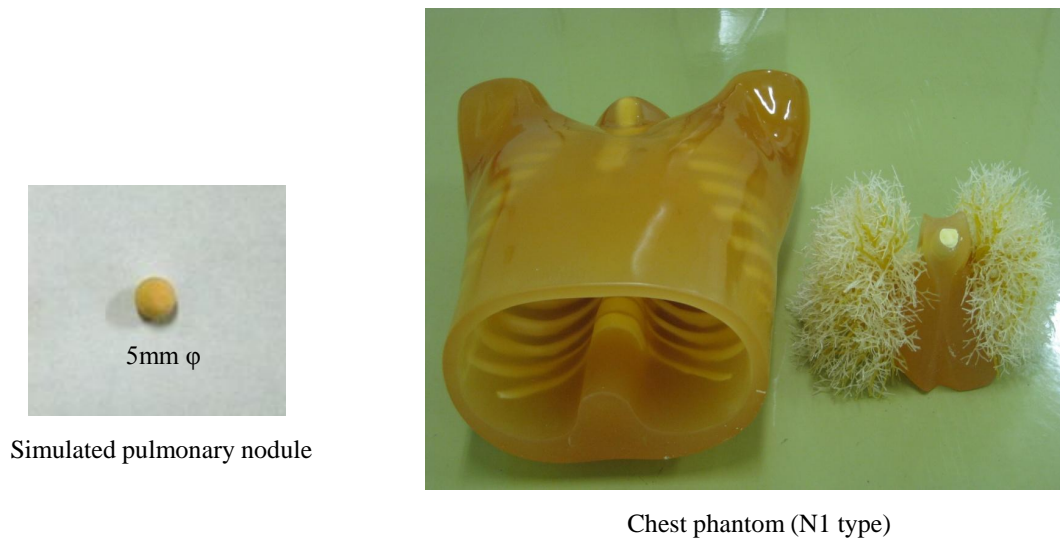
Chest phantom (N1 type)

Fig. (2). Illustration of the chest phantom (N1 type) and simulated pulmonary nodules.

different concentrations of hydroxyapatite were painted on the surface of the glass disks that have the same size. The calcifications are associated closely enough with the nodules so that they wind up in the same reconstructed slice.

2.3. Evaluation of SNR

The calcifications in the simulated pulmonary nodules were arranged in the lung region (right middle lobe position). Our analysis took into account the signal-to-noise ratio (SNR) of the different degrees of calcification in the simulated pulmonary nodules. Reconstruction kernel [20] was used of 5 filter types (edge enhance -- (very smooth), - (smooth), -+ (standard), + (slight sharp), ++ (sharp)). DES-DT techniques, such as signal-to-noise ratio (SNR) for the phantom study were evaluated.

The SNR is defined as $(N_1 - N_0)/\sigma_0$, where N_1 is the mean pixel value in the line within the region of calcification, N_0 is the mean pixel value in the line in a background area, and σ_0 is the standard deviation of pixel values in the base line. Throughout these results, σ_0 includes structure noise that can obscure the object, not just photon statistics and electronic noise.

2.4. Observer Study

Five thoracic radiologists evaluated the images for the presence of simulated pulmonary nodules by using the receiver operating characteristic (ROC) paradigm. We examined 30 samples with and 30 samples without different degrees of simulated pulmonary nodules with calcifications by both DES-DT and conventional digital tomosynthesis. The simulated pulmonary nodules were arranged in the lung region (random arrangement in a lung field area). Each case occurred only once in each group. The location of the nodules were somehow determined by a random number generator, which was also used to determine reading order. The readers presented with just the important slice. The readers presented both the conventional digital tomosynthesis and DES-DT images at different times. The observers were allowed to change window width and window level and use the pan and zoom functions. Before each session, two image sets of the 10 educational cases.

Each observer was instructed to detect simulated pulmonary nodules using a DES-DT images and conventional digital tomosynthesis images, and to separately describe the presence of a simulated pulmonary nodule using a continuous scale from 1 to 100. For simulated pulmonary nodules with calcifications, the score 100 represented the highest degree of confidence (probably a calcification) and score 0 represented the lowest degree of confidence (probably not a calcification). The time frame between reading the images was 1-2 weeks. Because of the large difference in appearance between the tomosynthesis images and the radiographs, this procedure was considered enough to avoid recall bias. ROC analysis software was used DBM MRMC Version 2.2 [21]. The detectability of the simulated pulmonary nodules was described by the area under ROC curves [22, 23]. For statistical analysis, the averaged area under the curve (AUC) and standard deviation were obtained by individually fitting ROC curves to the confidence ratings of each observer and averaging the estimated areas across observers. AUC values were used to test the significance of the differences by means of the paired F-test.

3. RESULTS

Evaluation of the SNR for DES-DT processing was investigated as shown in Figs. (**3**, **4**); for DES-DT processing were investigated as shown. DES-DT processing of the high-contrast detectability phantom case having clear contrast detectability produced an increase in same plane images. From results of SNR by a reconstruction filter, we realize that DES-DT is easy to detect calcification in comparison with conventional digital tomosynthesis when use an edge enhancement filter. In addition, a SNR value rise and a good correlation were present when DES-DT raised edge enhancement ratio when compared with conventional digital tomosynthesis. In this result, use of an edge enhancement filter is recommended for the detection of calcifications.

Based on the results of ROC performance analysis (Table **1**), the detection ability of our DES-DT was significantly better than that of conventional digital tomosynthesis (p < 0.03). ROC analysis was easy suffered from the tendency that DES-DT easy to detect in the case of amount of large
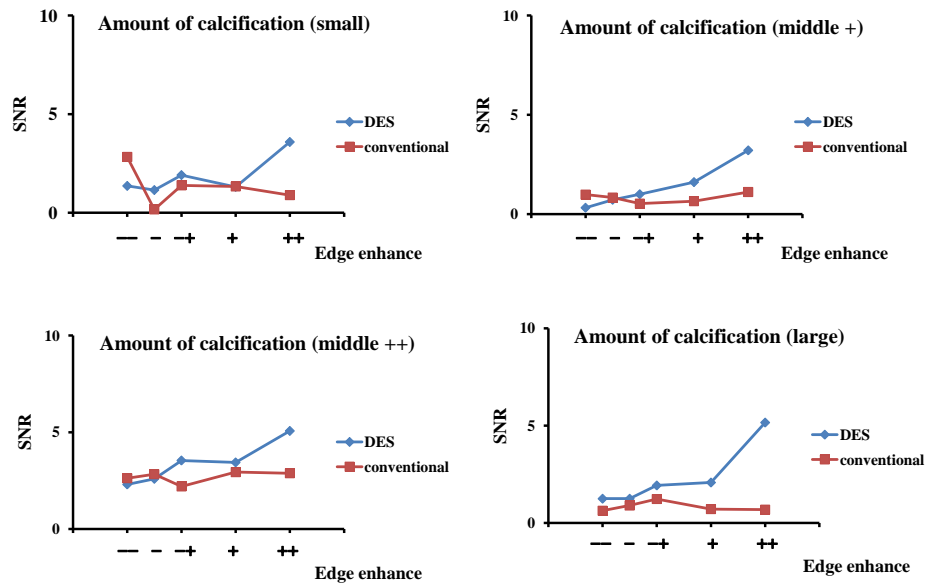
Fig. (3). Effect on SNR from a difference in reconstruction filter. It can confirm that SNR value increases when use a making edge enhancing filter. In addition, a dual-energy subtraction tomosynthesis processing can confirm that SNR value becomes high without coming to calcification content by amount.
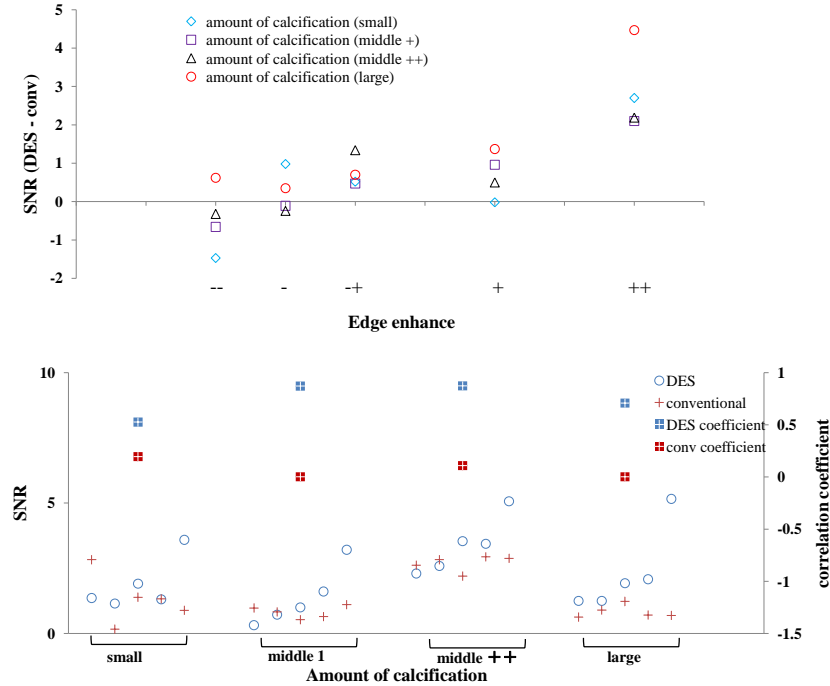

Fig. (4). (Top) A difference of a reconstruction filter and relationship of a SNR difference (It subtract SNR value of conventional digital tomosynthesis from SNR value of DES-DT). It can confirm that a difference of SNR value becomes large when use a making edge enhancing filter.

(Bottom) Relationship of SNR by a difference of the calcification content by amount that took five reconstruction filters into account. It can confirm that correlative between both sides because SNR value increases when calcification content by amount increases in DES processing.

calcification. We suffered from the results that significant difference produced in detectability by amount of calcification in an observer experiment. We indicated the potentiality that the detection was impossible in the case of amount of rare calcification. From a judgment basis between observers not having a change difference either, we can judge reliability of these experimental results. However, the significant difference was not accepted for detection with both in the case of amount of a little

calcification. We expect that a calcification may be buried all over the rippled pattern. We can expect to improve small amount of calcification detection if can exclude effect of rippled pattern.

4. DISCUSSION

The most reliable signs for discriminating between benign and malignant masses are the growth rate of the mass and the presence or absence of calcifications within the

Table 1. **The Comparison of Area Under the Curve (AUC) for Conventional and Dual-Energy Subtraction Tomosynthesis for the Observers. The Uncertainty Bars Represent 95% Confidence Intervals. (✽ CI; Confidence Interval)**
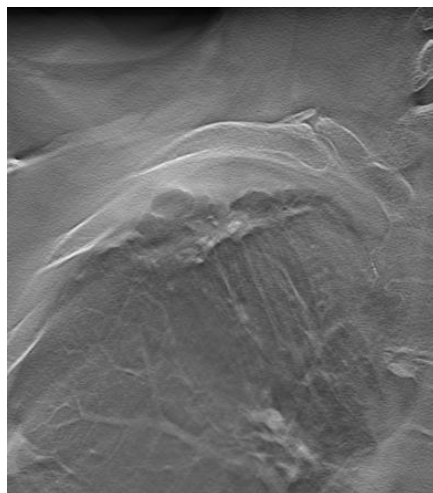
	calcifications (Small)		calcifications (Middle/Large)	
	DES	Conventional	DES	Conventional
Observer 1	0.841	0.883	0.964	0.882
Observer 2	0.917	0.875	0.987	0.919
Observer 3	0.980	0.835	1.000	0.878
Observer 4	0.912	0.930	1.000	0.964
Observer 5	0.874	0.882	0.965	0.949
Mean	0.905	0.881	0.983	0.918
Difference	0.024		0.065	
95% CI	[-0.0865 0.1337]		[0.0055 0.1236]	
Significant	Not significant		Significant (p<0.03)	

mass. Approximately 50% of surgically respected benign masses show a benign pattern of calcifications, although large bronchogenic carcinoma may show small, eccentrically distributed calcifications. Since calcifications are commonly seen in benign masses and since no other radiographic characteristic is specific in characterizing masses, it is important to detect and characterize calcifications within lesions. Using DES-DT, the presence, distribution, and characteristics of calcifications in lung nodules can be assessed to an extent that is not possible with currently available CT imaging and projection-type DES techniques. In addition, this technique does not suffer from the problems of image overlap, partial volume effects, or shifting of the image plane.

Quantum noise plays an important role in the degradation of contrast resolution of radiographs. It increases inversely with the x-ray exposure and constitutes the dominant noise

source at low radiation exposure levels. Because of quantum noise, the technical factors used to reduce radiation dose in our system are limited to those levels usually employed in conventional tomography. However, synthesized tomograms can be obtained with the same technical factors used for radiography when the presence of quantum noise can be tolerated. Any calcifications are visible in the presence of the overwhelming "rippled" artifact on the DES-DT images. This artifact a consequence of the inherent misregistration between the low kVp image and the high kVp considering that the x-ray tube is moving continuously. In addition, we present clinical trial cases (investigational patient) from the same patient (Fig. **5**). Clinical trial cases were confirmed that a calcification may be buried all over the rippled pattern. Ripple occurs by a similar mechanism as blurring and is a result of the limited number of projections in a sweep. This artifact is caused by a high-contrast structure (ripple source) that is far outside the imaging plane and whose contribution

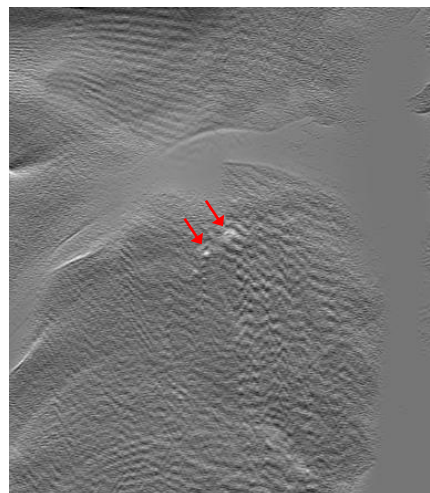**Tomosynthesis image (conventional)**   **Tomosynthesis image (DES)**

Fig. (5). Example of clinical trial examination case calcified tuberculous foci in 74-year-old male. Comparison of chest tomosynthesis images for the conventional digital tomosynthesis and dual-energy subtraction digital tomosynthesis.

to the plane in focus is not sufficiently blurred. In this situation, each interval between two successive projections, in the reconstructed image plane is wider than the tomographic blurring, so that separate images of the ripple source appear in the plane. Thus, blurring changes into ripple as the perpendicular distance from a ripple source to the plane in focus increases above a certain threshold.

The study compared of the ability of observers to detect simulated pulmonary nodules on DES-DT and conventional digital tomosynthesis images. Detection consisted of locating each perceived nodular opacity and assigning a level of confidence to its identification. The resulting plots of the true-positive fraction versus the mean number of false-positive fraction call per image indicated that for calcified, simulated nodules DES-DT performed significantly better (p < 0.03). Detection was improved because of several factors, but the ability of the DES method to remove quantum noise and its superior control of scatter were considered most important.

Initial data from our study suggest that DES-DT will substantially enhance sensitivity and specificity of pulmonary nodule detection. Despite its potential, DES-DT is a new technique. Therefore, there is no guidance for its integration into the clinical practice of conventional digital tomosynthesis. The most reliable signs for discriminating between benign and malignant masses are the growth rate of the mass and presence or absence of calcifications within the mass. Since calcifications are commonly observed in benign masses and no other radiographic characteristics is specific in characterizing masses, it is important to detect and characterize calcification within lesions. Using DES-DT, the presence, distribution, and characteristics of calcifications in lung nodules can be assessed to an extent that is not possible with currently available CT imaging and projection-type DES techniques. In addition, this technique is not susceptible to the problems of image overlap, partial volume effect, or shifting of the image plane.

We conclude that our DES-DT method is superior to the conventional digital tomosynthesis methods in the detection of simulated pulmonary nodules with calcifications than that method for the conventional digital tomosynthesis methods. These study results confirmed with a further study to assess influence of reconstruction and filtering for detection of simulated nodules. We believe firmly that DES-DT imaging quality can facilitate the detection of calcifications in pulmonary nodules.

REFERENCES

[1] Yankelevitz DF, Reeves AP, Kostis WJ, Zhao B, Henschke CI. Small pulmonary nodules: volumetrically determined growth rates based on CT evaluation. Radiology 2000; 217: 251-6.

[2] Brody WR, Butt G, Hall A, Macovski A. A method for selective tissue and bone visualization using dual-energy scanned projection radiography. Med Phys 1981; 8: 659-67.

[3] Lehmann LA, Alvarez RE, Macovski A, *et al.* Generalized image combinations in dual KVP digital radiography. Med Phys 1981; 8: 659-67.

[4] Kruger RA, Armstrong JD, Sorenson JA, Niklason LT. Dual energy film subtraction technique for detecting calcification in solitary pulmonary nodules. Radiology 1981; 140: 213-9.

[5] Godwin JD. The solitary pulmonary nodule. Radiol Clin North Am 1983; 21: 709-21.

[6] Littleton JT. Pluridirectional tomography in diagnosis and management of early bronchogenic carcinoma. In: sectional imaging methods. A comparison, University Park Press, ML, pp 155; 1983.

[7] Siegelman SS, Khouri NF, Leo FP, Fishman EK, Rraverman RM, Zerhouni EA. Solitary pulmonary nodules. CT assessment. Radiology 1986; 160: 307-12.

[8] Siegelman SS, Zerhouni EA, Loe FP, Khouri NF, Stitik FP. CT of the solitary pulmonary nodule. AJR 1980; 135: 1-13.

[9] Zerhouni EA, Caskey C, Khouri NF. The pulmonary nodules. Semin Ultrasound CT MR 1988; 9: 67-78.

[10] Fraser RG, Hickey NM, Niklason LT, *et al.* Calcification in pulmonary nodules. detection with dual-energy digital radiography. Radiology 1986; 160: 595-601.

[11] McLendon RE, Roggli VL, Foster WL Jr, Becsey D. Carcinoma of the lung with osseous stromal metaplasia. Arch Pathol Lab Med 1985; 109: 1051-3.

[12] O'Keefe ME Jr, Good CA, McNonald JR. Calcification in solitary nodules of the lung. AJR 1957; 77: 1023-33.

[13] Siegelman SS, Zerhouni EA. Computed tomography of the solitary pulmonary nodule. In: Sectional imaging methods. A comparison, University Park Press, ML 1983; pp. 175-82.

[14] Burgener FA and Kormano M. Differential diagnosis in conventional radiology. Thieme, Berlin; 1991.

[15] Hickey NM, Niklason LT, Sabbagh E, Fraser RG, Barnes GT. Dual-energy digital radiographic quantification of calcium in simulated pulmonary nodules. AJR 1987; 148: 19-24.

[16] Ishigaki T, Sakuma S, Horikawa Y, Ikeda M, Yamaguchi H. One-shot dual-energy subtraction imaging. Radiogy 1986; 161: 271-3.

[17] Ishigaki T, Sakuma S, Ikeda M. One-shot dual-energy subtraction chest imaging with computed radiography. Radiology 1988; 168: 67-72.

[18] Nishitani H, Umezu Y, Ogawa K, Yuzuriha H, Tanaka H, Matsuura K. Dual-energy projection radiography using condenser X-ray generator and digital radiography apparatus. Radiology 1986; 161: 533-5.

[19] Dobbins 3rd JT, Godfrey DJ. Digital x-ray tomosynthesis: curent state of the art and clinical potential. Phy Med Biol 2003; 48: R65-106.

[20] Gomi T, Hirano H. Clinical potential of digital linear tomosynthesis imaging of total joint artroplasty. J Digit Imaging 2008; 21: 312-22.

[21] Berbaum K. DBM MRMC software 2.2. URL: http://perception.-radiology.uiowa.edu (published June 24, 2008; accessed January 7, 2009).

[22] Hanley JA, McNeil BJ. The meaning and use of the area under receiver operating characteristic (ROC) curves. Radiology 1982; 143: 29-36.

[23] Hanley JA, McNeil BJ. A method of comparing the areas under receiver operating characteristic curves derived from the same cases. Radiology 1983; 148: 839-843.